

Electrostatically-controlled protein adsorption onto lipid bilayer: Modeling adsorbate aggregation behavior

Valeriya M. Trusova*, Galyna P. Gorbenko

Department of Biological and Medical Physics, V.N. Karazin Kharkov National University, 4 Svobody Sq., Kharkov, 61077, Ukraine

Received 21 November 2007; received in revised form 19 December 2007; accepted 19 December 2007

Available online 27 December 2007

Abstract

Using adsorption models based on scaled particle (SPT) and double layer theories the electrostatically-controlled protein adsorption onto membrane surface has been simulated for non-associating and self-associating ligands. The binding isotherms of monomeric and oligomeric protein species have been calculated over a range of variable parameters including lipid and protein concentrations, protein and membrane charges, pH and ionic strength. Adsorption behavior of monomers appeared to be the most sensitive to the changes in the protein aggregation state. The hallmarks of the protein oligomerization are identified. The practical guides for optimal design of binding experiments focused on obtaining proofs of protein self-association are suggested.

© 2007 Elsevier B.V. All rights reserved.

Keywords: Protein adsorption; Lipid bilayer; Protein aggregation

1. Introduction

During the last decade the phenomenon of protein aggregation attracts considerable attention due to its involvement in the etiology of a number of the so-called conformational diseases, including Alzheimer's, Parkinson's, Huntingtons diseases, type II diabetes, rheumatoid arthritis, spongiform encephalopathies (prion diseases) [1–3]. Accumulating evidence lends support to the hypothesis that the formation of abnormal protein aggregates *in vivo* can be driven by destabilization of the protein structure upon its adsorption at interfaces, formed by cellular membranes [2]. Lipid bilayer, a basic structural element of biological membranes, provides a unique environment favoring the structural transformation of polypeptide chain into partially folded conformation, protein accumulation at lipid-water interface, screening of the protein surface charge, modifications in hydrogen bonding capability of the adsorbed molecules, aggregation-favoring orientation of the bound protein, the processes which can ultimately lead to the protein

polymerization [2,4]. For these reasons increasingly growing efforts are currently focused on characterization of the aggregation properties of interfacially adsorbed proteins. While examining protein adsorption onto lipid bilayer it's naturally to expect that the binding curves *per se* would provide evidence for the changes in protein oligomerization state. Experimentally, the adsorption isotherms can be obtained by two main groups of assays [5]. The first group includes direct methods (gel filtration and centrifugation), which are based on physical separation of bound and free protein. Yet, these methods have serious drawbacks — they are time-consuming and separation may shift the equilibrium between free and bound species. The second group involves indirect spectroscopic methods based on relation between the change in a certain parameter (absorbance, fluorescence intensity, anisotropy, lifetime, efficiency of resonance energy transfer, etc.) and amount of bound protein. These methods allow tracking the adsorption behavior individually for bound monomers and oligomers provided that spectral responses of monomeric and self-associating species are different [6–9]. However, once the adsorption isotherm is obtained, it is difficult to discern what protein state (monomeric or oligomeric) is responsible for the characteristics of the experimental curve. A question arises whether the binding experiments can be

* Corresponding author. 66-82 Geroyev Truda St., Kharkov 61121, Ukraine. Tel.: +380 57 364 29 34, +380 57 343 82 44; fax: +380 57 705 00 96.

E-mail address: valtrusova@yahoo.com (V.M. Trusova).

Notation

K_a	Protein association constant
K_{1z}	Equilibrium constant for the formation of protein z_a -mer
F	Concentration of the protein free in solution
z_a	Degree of protein oligomerization
γ	Activity coefficient of adsorbed species
Φ	Fraction of surface area occupied by adsorbed protein
B_1, B_z	Concentrations of bound monomers and z_a -mers, respectively
B	Total concentration of bound protein
n	Number of lipid molecules covered by a single protein
L_a	Concentration of accessible for protein lipids
R	Radius of the circle representing protein species
ΔF_{el}	Total gain in electrostatic free energy
F_{el}^s, F_{el}^P	Electrostatic free energies of a membrane surface and a protein, respectively
z	Protein charge
κ	Reciprocal Debye length
c	Molar concentration of monovalent ions
S_L	Mean area per lipid molecule
f_{PC}, f_A	The mole fractions of phosphatidylcholine (PC) and acidic phospholipids, respectively
S_{PC}, S_A	Mean areas per PC and acidic phospholipid headgroups, respectively
σ	Bilayer surface charge density
α	Degree of anionic phospholipid ionization
$K^{(i)}$	Anionic phospholipid ionization constant
$[H^+]_b$	Bulk proton concentration
ψ_o	Membrane electrostatic surface potential
L	Total lipid concentration
P	Total protein concentration

Subscripts

(1)	protein monomer
(z)	protein z_a -mer

designed in a manner minimizing the uncertainty in data interpretation. One approach to answering this question is based on analysis of simulated binding data obtained over a range of parameters that can be varied in experiment. In the present paper, we treat the problem of membrane adsorption of self-associating protein making emphasis on the practical guides to planning and analyzing the results of binding studies. Our goal was several-fold: i) to analyze different types of adsorption isotherms; ii) to ascertain what characteristics of binding curve may be indicative of the changes in protein aggregation state; iii) to evaluate the possibility of choosing the set of experimental variables providing unambiguous proofs of the protein aggregation.

2. Theory

Protein adsorption onto membrane surface is characterized by a number of peculiar features associated, particularly, with large size of ligand, steric area-excluding interactions between the adsorbing protein molecules, strong dependence of the binding process on a ligand shape, i.e. on geometrical arrangement of protein–lipid contacts. Theoretical description of the protein–membrane binding is provided by a series of lattice and con-

tinuum models of large ligand adsorption to membranes developed by Stankowski [10–12], Heimburg & Marsh [13], Chatelier & Minton [14], Talbot [15], Al-Malah [16], Wahlgren et al. [17]. In terms of the lattice models lipid bilayer is considered as a regular array of binding contacts (subunits), forming the protein binding sites according to the size and shape of contact region [10–12]. Continuum models treat protein adsorption to a surface on a basis of scaled-particle theory (SPT) [14,15,18]. SPT is based on deriving the chemical potentials of hard convex particle fluid through calculating the work necessary for adsorption of a scaled particle on a surface. SPT is currently regarded as providing most adequate description of excluded area interactions between the adsorbing protein molecules. To date, a formalism of SPT model is developed for the cases of adsorption of large ligands of various shape on a surface [10,11], cooperative binding [12], adsorbate incorporation into a membrane [12], competition between two large ligands [14], self-association of a surface-bound protein [14], multiple adsorbate conformations [18].

In the present work we applied two-state SPT model of self-associating ligand proposed by Minton [14] to simulate the membrane adsorption of cationic peripheral proteins. Since the

process is predominantly electrostatic in nature, we extended Minton's SPT model to take into account not only area exclusion, but also electrostatic effects. The two-state model assumes that adsorbed protein exists only in two states — monomer and z_a -mer. In this case the adsorption isotherm is given by:

$$K_a F = \Phi_1 \gamma_1(\Phi_1, \Phi_z) \quad (1)$$

$$\Phi_z = z_a K_{1z} \frac{\gamma_1(\Phi_1, \Phi_z)^{z_a}}{\gamma_z(\Phi_1, \Phi_z)} \Phi_1^{z_a} \quad (2)$$

$$\ln \gamma_1 = -\ln(1 - \Phi) + \frac{3\Phi_1 + \left[\frac{2}{q} + \frac{1}{q^2}\right]\Phi_z}{1 - \Phi} + \frac{\left(\Phi_1 + \frac{1}{q}\Phi_z\right)^2}{(1 - \Phi)^2} \quad (3)$$

$$\ln \gamma_z = -\ln(1 - \Phi) + \frac{3\Phi_z + (2q + q^2)\Phi_1}{1 - \Phi} + \frac{(\Phi_z + q\Phi_1)^2}{(1 - \Phi)^2} \quad (4)$$

where $\Phi_1 = nB_1/L_a$, $\Phi_z = nB_z/L_a$, $L_a = 0.5 L$, $\Phi = \Phi_1 + \Phi_z$, $q = R_z/R_1$. For the case of conserved area upon self-association $q = z_a^{1/2}$. The equilibrium binding constant is generally represented as consisting of electrostatic (K_{el}) and intrinsic non-electrostatic (K_o) terms: ($K_a = K_{el}K_o$). Adequate description of electrostatically-driven protein adsorption onto lipid bilayer requires allowing for dependence of association constant on membrane electrostatic potential or surface charge density. The latter, in turn, is a function of mole fraction of anionic phospholipids, pH, ionic strength and extent of protein binding (surface coverage) [13].

Electrostatic component of the binding constant is given by [13]:

$$K_{el} = \exp\left(-\frac{d}{dN_P} \left[\frac{\Delta F_{el}(N_P)}{k_B T} \right]\right) \quad (5)$$

where T is the temperature, k_B is Boltzmann's constant, and ΔF_{el} is a function of the number of adsorbed protein molecules, $N_P = BN_A$:

$$\Delta F_{el}(N_P) = F_{el}^s(N_P) - F_{el}^s(0) - N_P F_{el}^P. \quad (6)$$

The electrostatic free energy of a spherical protein molecule with effective charge $+ze$, radius r_o and uniform charge distribution can be written as [19]:

$$F_{el}^P = \frac{z^2 e^2}{2\epsilon r_o (1 + \kappa r_o)} \quad (7)$$

$$\kappa = \sqrt{\frac{8\pi e^2 N_A c}{\epsilon k_B T}} \quad (8)$$

with e being the elementary charge, N_A is Avogadro's number, ϵ is the dielectric constant. In terms of the Gouy–Chapman double layer theory the electrostatic free energy of a membrane of area $S_m = S_L L_a$ is given by [20]:

$$F_{el}^s = \frac{2k_B T S_m}{e} \left(\sigma \sinh^{-1} \left(\frac{\sigma}{a} \right) - \sqrt{a^2 + \sigma^2} + a \right); \quad (9)$$

$$a = \sqrt{2\pi^{-1} \epsilon c N_A k_B T}$$

where $S_L = (f_{PC} S_{PC} + f_A S_A)$.

σ is given by:

$$\sigma = \frac{-e(\alpha f_A L_a - zB)}{S_m} \quad (10)$$

In the case of one-step deprotonation α can be written as:

$$\alpha = \frac{K^{(i)}}{K^{(i)} + [H^+]_b \exp\left(\frac{-e\psi_o}{k_B T}\right)}. \quad (11)$$

Electrostatic surface potential of a membrane related to the surface charge density is defined as:

$$\psi_o = \frac{2k_B T}{e} \sinh^{-1} \left(\frac{\sigma}{a} \right) \quad (12)$$

Numerical solution of the set of Eqs. (1)–(12) yields theoretical adsorption isotherms.

3. Results and discussion

3.1. General shape of adsorption isotherms upon formation of protein aggregates

While examining protein–lipid complexation several types of binding curves can be obtained in an experiment, viz. dependencies of concentrations of various bound species (monomers (B_1) and oligomers (B_z)) and whole protein ($B = B_1 + z_a B_z$) either on protein (P) or lipid (L) concentration. First, it seems of interest to ascertain how the shape of adsorption isotherms depends on degree of oligomerization. Fig. 1 represents a set of adsorption isotherms calculated at varying L and constant P ($P = \text{const}$, $L = \text{var}$). The following salient features of the binding curves should be pointed out:

- bound monomers* (Fig. 1, A) — the shape of adsorption isotherms changes from Langmuir-like to sigmoidal at $z_a > 2$, point of inflexion increases with z_a . Sigmoidal curves are characterized by initial “lag region” (lipid concentrations from 0 to $\sim 4 \mu\text{M}$) which correlates with accumulation of bound oligomers;
- bound oligomers* (Fig. 1, B) — adsorption curves have asymmetric bell-shaped form with the maximum at certain lipid-to-protein molar ratio ($L:P$) (in our case ≈ 27). Notably, asymmetry rises with z_a ($z_a \rightarrow \infty$, $B_z \rightarrow B$);
- bound protein* (monomers+oligomers) (Fig. 1, C) — adsorption curves have typical Langmuir-like shape with the steepness increasing and saturation point decreasing with the degree of oligomerization (as predicted for co-operative process).

As seen in Fig. 2, in the case of fixed lipid and varied protein concentration ($L = \text{const}$, $P = \text{var}$) the adsorption isotherms exhibit somewhat different behavior:

- bound monomers* (Fig. 2, A) — in the absence of oligomerization ($z_a = 1$) the binding curve is Langmuir-like, while upon protein self-association ($z_a \geq 2$) it

converts into the asymmetric bell-shaped isotherm. Maximum position depends on the degree of oligomerization, being observed at $L: P=33, 50, 83, 135$ for $z_a=1, 2, 4, 8$, respectively.

- ii) *bound oligomers* (Fig. 2, B) — the isotherms have sigmoidal shape, concentration of bound aggregates rises with z_a , point of inflexion decreases with z_a .
- iii) *bound protein* (Fig. 2, C) — the isotherms have Langmuir-like shape. Notable point — all curves initially coincide at low protein concentrations (0–0.5 μM), while at $P>0.5 \mu\text{M}$ — the higher degree of oligomerization, the longer linear region in the binding isotherm. In other words, increase in z_a is coupled with the elevated saturation level.

One extremely important point should be stressed. Simulation results demonstrate that formation of protein oligomers can be recognized only by examination of adsorption isotherms for monomers undergoing characteristic changes (from Langmuir-like to sigmoidal ($P=\text{const}$, $L=\text{var}$) or asymmetric bell-shaped ($L=\text{const}$, $P=\text{var}$)) with increasing degree of oligomerization. In the meantime, the shape of binding curves both for oligomers and whole protein remains virtually invariant upon protein aggregation. Further analysis of simulation data revealed another hallmark of the protein oligomerization. As indicated above, the adsorption isotherms $B(L)$ ($P=\text{const}=0.15 \mu\text{M}$) have saturation points differing for $z_a=1$ and $z_a \geq 2$ (Fig. 1, C). However, when P was increased up to 0.5 and 1 μM , the $L:P$ value, corresponding to saturation, decreased for $z_a=1$ and remained virtually unchanged for $z_a=4$ (Fig. 3). This implies that comparing the saturation points for adsorption isotherms $B(L)$ obtained at different P may yield additional proof for protein aggregation.

3.2. Effect of protein and membrane charges on the behavior of adsorption curves

At the next step of the study we addressed the question of whether the presence of protein oligomers could affect charge-dependent characteristics of the adsorption isotherms. Experimentally, protein charge can be modified, for instance, by substitution of certain charged amino groups or covalent labeling of protein. In turn, charge of lipid bilayer surface is easily controlled by varying the proportion of anionic phospholipid.

Concentrating on Fig. 4, it is clearly seen that concentration of bound monomers increases with increasing protein charge from 2 to 8. In the absence of oligomerization the B_1 rise is coupled with increase in steepness of binding curves (Fig. 4, A), while at $z_a=4$ changes in protein charge provoke modifications in the shape of isotherms (Fig. 4, B), viz. their conversion from sigmoidal ($z=2, 4, 6$) to Langmuir-like ($z=8$). Qualitatively this effect may be explained as follows. Lateral protein-protein interactions, which result in the formation of protein self-assemblies, become possible due to protein charge screening by anionic lipid headgroups in the interaction zone. Evidently, at relatively low z (≤ 6) charge

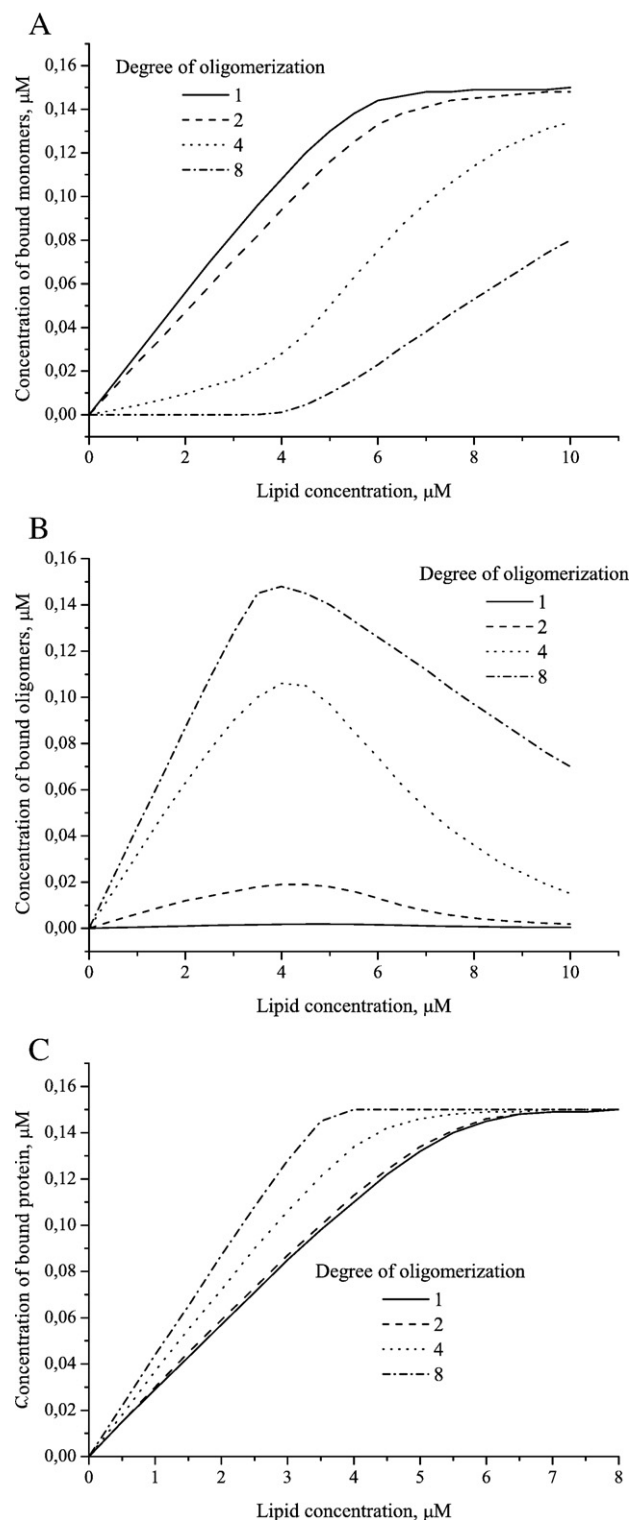


Fig. 1. Adsorption isotherms of bound monomers (A), oligomers (B) and whole protein (C) at different degree of oligomerization in the case of fixed protein concentration (0.15 μM) and varied lipid concentration. The curves are calculated with the following values of model parameters: $n=10$, $K_0=10 \mu\text{M}$, $K_{12}=0.1$, $z=4$, $f_A=0.4$, $c=20 \text{ mM}$, $\text{pH}=7.4$.

neutralization may prove sufficient for protein self-association. However, at higher z , for instance, $z=8$, protein charge neutralization by lipids is appeared much less, so that protein-

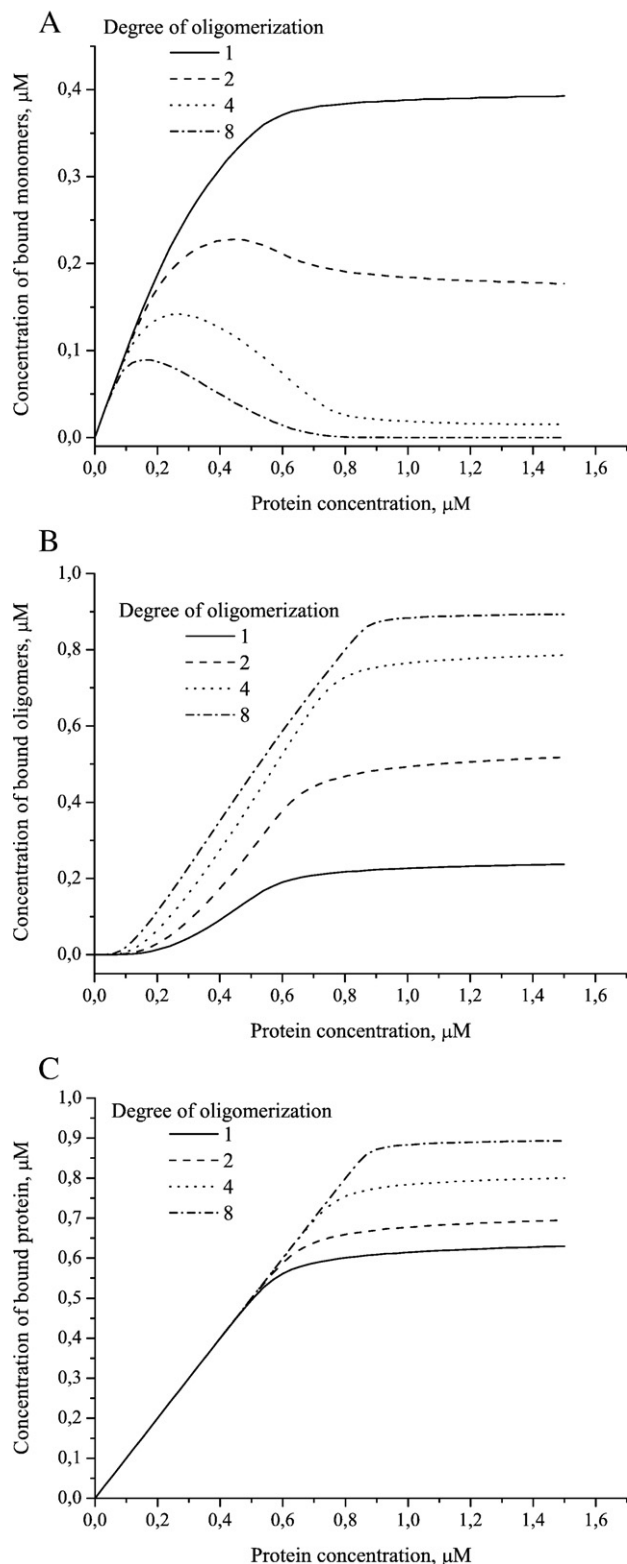


Fig. 2. Binding curves for monomers (A), oligomers (B) and whole protein (C) at different degrees of oligomerization in the case of constant lipid concentration (20 μM) and varied protein concentration. The fitting parameters are: $n=10$, $K_0=10$ μM, $K_{1z}=0.1$, $z=4$, $f_A=0.4$, $c=20$ mM, $\text{pH}=7.4$.

protein repulsions would hinder aggregate formation. In this case concentration of oligomers significantly decreases (Fig. 4, C), and monomer adsorption isotherm becomes

insensitive to the presence of protein aggregates (Fig. 4, B). This example demonstrates that Langmuir-like shape of experimental isotherm is not necessarily indicative of the absence of protein oligomerization. Test for dependency of isotherm shape on the protein charge may be more definitive.

Notably, effect on protein charge on the behavior of monomer adsorption isotherms in the case of varying P and fixed L was nearly the same — at $z_a=1$ rise in z brings about only enhancement of monomer binding (Fig. 5, A), whereas at $z_a=4$ $B_1(P)$ dependencies undergo transformation from asymmetric bell-shaped to Langmuir-like form (Fig. 5, B) providing additional arguments to the suggestion about reduced sensitivity of monomer adsorption curves to the presence of oligomers at high protein charge ($z>6$).

Meanwhile, somewhat unexpected behavior was revealed for the $B(P)$ dependencies. Conceptually, enhancement of electrostatic protein–lipid interactions with rising z would result in the increase of bound protein concentration. This was observed in the absence of oligomerization (Fig. 5, C) but not in the case of $z_a=4$ where increasing protein charge was followed by remarkable decrease in B (Fig. 5, D). Mathematically, this phenomenon is likely to reflect a superposition of opposite changes in concentrations of bound monomers and oligomers with increase in z . More specifically, B_1 exhibited about two-fold increase with elevating z (Fig. 5, B) while changes in concentration of bound oligomers were much more pronounced — B_z decreased by a factor of 4 at $z_a=4$ upon rising the protein charge from 4 to 8 (data not shown). Dominating drop in B_z results, obviously, in overall decrease in total concentration of bound protein (Fig. 5, D).

The strength of electrostatic protein–lipid interactions can be also modulated by lipid bilayer surface charge density. At $z_a=1$ all kinds of adsorption isotherms were featured by enhancement of protein–membrane binding upon increasing the content of anionic phospholipid (Table 1). On the contrary, in the case of protein aggregation the behavior of binding curves was more

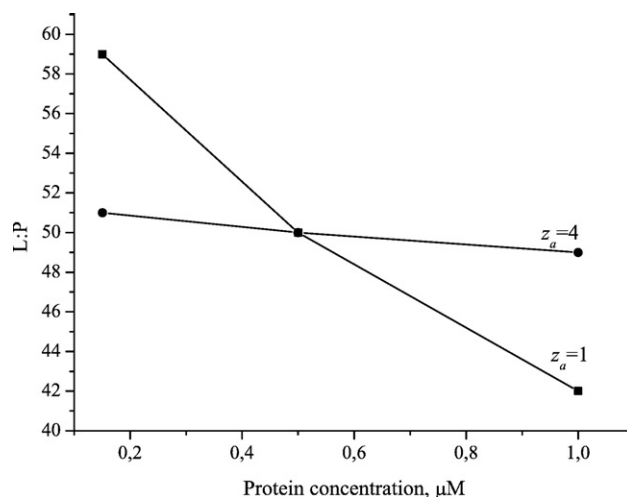


Fig. 3. Lipid-to-protein molar ratios corresponding to saturation point of $B(L)$ adsorption isotherms calculated for different P (0.15, 0.5 and 1 μM). The model parameters were $n=10$, $K_0=10$ μM, $K_{1z}=0.1$, $z=4$, $f_A=0.1$, $c=20$ mM, $\text{pH}=7.4$.

complex. Specifically, at $z_a=4$ adsorption isotherms exhibited the following peculiarities:

- i) *bound monomers* (Fig. 6, A, D) — the curves change their shape from Langmuir-like to sigmoidal ($P=\text{const}$, $L=\text{var}$) or to asymmetric bell-shaped ($L=\text{const}$, $P=\text{var}$) with the rise in bilayer surface charge density;
- ii) *bound oligomers* (Fig. 6, B) — B_z significantly increases upon increase in anionic lipid content with the maximum position being dependent on f_A ;
- iii) *bound protein* (Fig. 6, C) — B increases, and $L:P$, corresponding to saturation point, decreases with f_A .

It can be assumed that the observed behavior of monomer adsorption isotherms (Fig. 6, A, D) is a result of prevailing role of K_{el} (strongly determined by bilayer surface charge density (Eqs. (5)–(9))) in determining the shape of binding curves. At this point it should be noted that K_{el} (and, as a consequence, K_a) tends to increase with lipid concentration and decrease with protein concentration as illustrated in Fig. 7. These tendencies reflect alterations in the extent of membrane charge neutralization by the adsorbed protein. However, electrostatically-controlled increase of association constant proved insufficient to explain the changes of isotherm shape occurring upon increasing the mole fraction of anionic phospholipid. Furthermore, simple increasing the value of K_o and K_{1z} didn't result in sigmoidal $B_1(L)$ (or bell-shaped $B_1(P)$) dependencies at f_A not exceeding 0.2. Accordingly, the recovered change of monomer adsorption isotherms is unlikely to have a mathematical origin, and presumably stems from the strengthening of protein aggregation propensity with increasing membrane charge. It seems reasonable to assume that in the case of weakly charged membrane the concentration of bound oligomers is not enough (Fig. 6, B) to provide the sigmoidal shape of binding curves of monomeric species. In contrast, at high content of anionic phospholipid significant enhancement of electrostatic binding component favors the protein accumulation at lipid-water interface thereby facilitating its aggregation. This manifests itself not only in the increase in B_z but also in the conversion of monomer adsorption isotherm from Langmuir-like to sigmoidal or bell-shaped (Fig. 6, A, D). The assumption about strengthening of protein aggregation propensity upon increasing membrane charge is also corroborated by the finding that the higher f_A , the lower $L:P$ corresponding to the maximum concentration of bound oligomers (Fig. 6, B).

Importantly, the above phenomenon may have direct biological relevance. The structure of natural membranes is known to be highly heterogeneous. The factors such as temperature [21], lipid–lipid [22] or lipid–protein [23] hydrophobic mismatch, enzymatic cleavage of lipids [24], surface electrostatic associations [25], or hydrogen bonding between lipid headgroups [26] may give rise to laterally separated phases within bilayer. A number of studies indicated heterogeneous lipid organization to control the binding of charged macromolecules [23,25]. The protein adsorption onto different lipid lateral domains varying in lipid composition and charge may modulate its aggregation propensity. Furthermore, protein binding *per se*

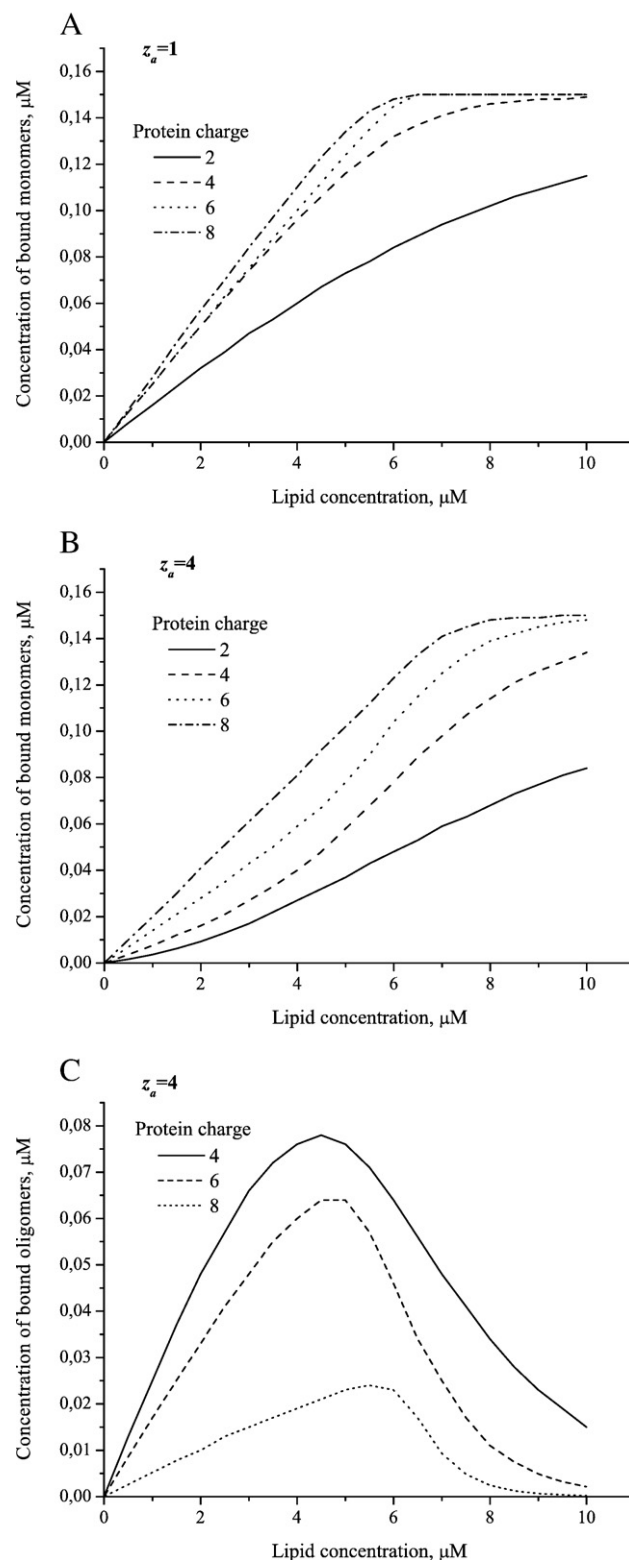


Fig. 4. Protein charge effect on the shape of monomer (A, B) or oligomer (C) adsorption isotherms at different z_a for varied lipid concentrations, $n=12$, $K_o=10$ μM, $K_{1z}=0.1$, $f_A=0.4$, $c=20$ mM, pH=7.4, $P=0.15$ μM.

may cause the formation of lipid domains [27–31]. The extent of protein-induced lipid segregation is thought to be dictated by the minimum of the total interaction free energy reflecting the

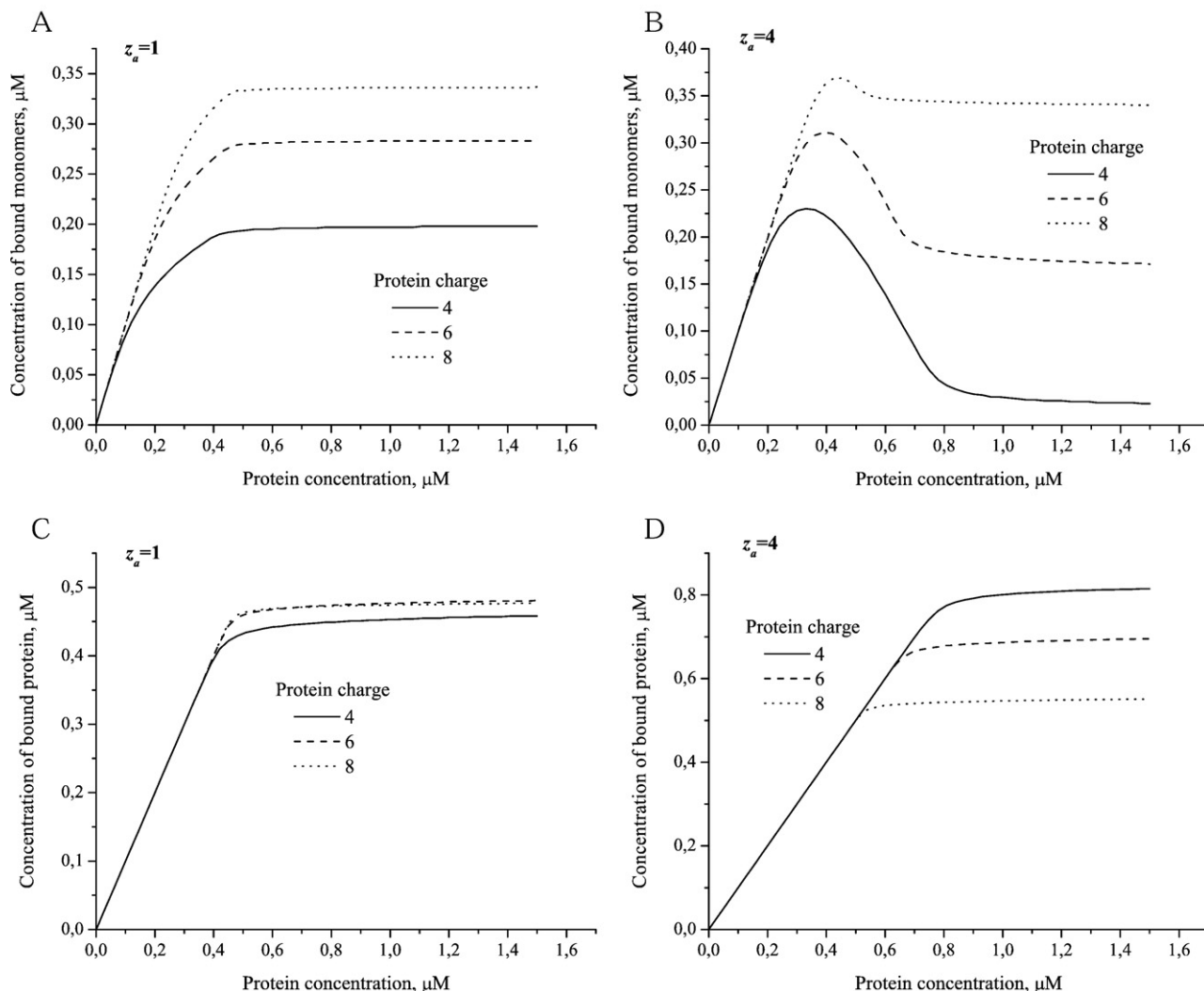


Fig. 5. Concentration of bound monomers (A, B) and whole protein (C, D) as a function of P at different values of protein charge. The fitting parameters are: $n = 12$, $K_0 = 10 \mu\text{M}$, $K_{12} = 10$, $L = 20 \mu\text{M}$, $f_A = 0.4$, $c = 20 \text{ mM}$, $\text{pH} = 7.4$.

balance between the gain in electrostatic adsorption energy and the loss of lipid mixing entropy. The models for domain formation emphasize the importance of both electrostatic and nonelectrostatic mechanisms, involving lipid-mediated attraction between adsorbed proteins coupled with elastic membrane deformation.

3.3. Influence of pH and ionic strength on the behavior of adsorption isotherms

In the following, it seems of interest to assess whether the modifications of adsorption isotherms in response to the changes in pH or ionic strength could be indicative of protein oligomerization. Presented in Fig. 8 are the results of numerical simulation obtained at varying pH. When P was set constant, increasing pH from 3 to 8 units was followed by the enhancement of monomer binding and steepening of the isotherms at $z_a = 1$, and curve conversion from Langmuir-like to sigmoidal at $z_a = 4$ (Fig. 8, A, B). For $B_2(L)$ and $B(L)$ dependencies the rise in pH resulted only in B_2 and B increase

without any changes in curve shape (Table 1). Note that all the above calculations have been made with $\text{p}K_a$, the value corresponding to ionization constant of phosphatidylglycerol. The shape of monomer adsorption isotherms at $z_a = 4$ seems to be controlled by the differences between pH and $\text{p}K_a$. Thus, while interpreting the experimental results, one should bear in mind that Langmuir-like $B_1(L)$ dependencies is not the evidence of protein weakened aggregation propensity, and may result from small $|\text{pH} - \text{p}K_a|$ but not from the absence of protein oligomers. Hence, the experimental conditions should be chosen to ensure sufficient difference between ionization constant of anionic lipid and pH of buffer solution. It should be noted that ionization constant of anionic phospholipids falls in a wide range from 2.5 (phosphatidylinositol) to 5.5 (phosphatidylserine) [32]. Situation proves much more complex when bilayer anionic constituent is represented by phospholipid undergoing two-step deprotonation like cardiolipin. This lipid, containing two phosphate groups and four acyl chains, has two widely separated $\text{p}K_a$ values — one at 2.8 and a second between 7.5 and 9.5 [33]. In this case, the shape of $B_1(L)$ curves seems to be

Table 1
Effect of protein aggregation on characteristics of adsorption isotherms calculated over a range of variable parameters

Variable parameter	Characteristic features of adsorption isotherms observed at increasing variable parameter					
	Monomers		Oligomers		Whole protein	
	$P=\text{const}, L=\text{var}$	$L=\text{const}, P=\text{var}$	$P=\text{const}, L=\text{var}$	$L=\text{const}, P=\text{var}$	$P=\text{const}, L=\text{var}$	$L=\text{const}, P=\text{var}$
	$B_1 \downarrow^a$ with \uparrow in z_a		$B_z \uparrow$ with z_a			
z	$z_a=1$: \uparrow in curve steepness, $z_a=4$: isotherm conversion from ss to Ll with \uparrow in z . $B_1 \uparrow$ with z	$z_a=4$: curve conversion from bs to Ll with \uparrow in z .	Asymmetric bs, maximum position shifts towards higher L:P with \uparrow in z $B_z \downarrow$ with \uparrow in z	Invariant ss form at all z	Invariant Ll form at all z independent of z_a , \uparrow in B and curve steepness with z	Invariant Ll form at all z independent of z_a , $z_a=1$: $B \uparrow$ with z , $z_a=4$: $B \downarrow$ with z
f_A	$z_a=1$: \uparrow in B_l and curve steepness, $z_a=4$: isotherm conversion from Ll to ss with \uparrow in f_A	$z_a=1$: Ll form, \uparrow in B_l , $z_a=4$: isotherm conversion from Ll to bs, \downarrow in B_l with \uparrow in f_A	Asymmetric bs, maximum position shifts towards lower L:P with \uparrow in f_A $B_z \uparrow$ with f_A	ss at all f_A	Ll form at all f_A independent of z_a , \uparrow in steepness with f_A $B \uparrow$ with f_A	Invariant Ll form at all f_A , no dependency on z_a
pH	$z_a=1$: L.-l. form, \uparrow in B_l and curve steepness, $z_a=4$: isotherm conversion from Ll to ss with \uparrow in pH	$z_a=1$: Ll, \uparrow in B_l , $z_a=4$: bs form, \downarrow in B_l with \uparrow in pH	Asymmetric bs, maximum position is independent of pH $B_z \uparrow$ with pH	ss at examined range of pH	Ll form at all pH independent of z_a , \uparrow in steepness with pH $B \uparrow$ with pH	Ll form at all pH independent of z_a
c	$z_a=1$: Ll form, \downarrow in B_l and curve steepness, $z_a=4$: isotherm conversion from ss to Ll with \uparrow in c	$z_a=1$: Ll, \downarrow in B_l , $z_a=4$: bs form, \uparrow in B_l with \uparrow in c	Asymmetric bs, maximum position shifts towards higher L:P with \uparrow in c $B_z \downarrow$ with \uparrow in c	ss at examined range of c	Ll form at all c independent of z_a , \downarrow in steepness with \uparrow in c $B \downarrow$ with \uparrow in c	Ll form at all c independent of z_a

Highlighted in grey are characteristic features of adsorption isotherms which can be treated as manifestation of protein oligomerization.

ss — sigmoidal shape, bs — bell-shaped, Ll — Langmuir-like shape.

^a Upward and downward arrows denote increase and decrease of certain parameters, respectively.

controlled not only by $|\text{pH}-\text{pK}_a|$ difference but also by the balance between deprotonated and partially protonated cardiolipin species.

However, one should bear in mind that we didn't consider protein charge as a function of pH. In real systems, isoelectric point of the protein under study determines z dependency on pH, and binding curves may reflect the contribution from $|\text{pH}-\text{pK}_a|$ and $|\text{pH}-\text{pI}|$.

Analysis of adsorption isotherms calculated at varying pH and fixed lipid concentration revealed interesting behavior only for $B_1(P)$ at $z_a=4$ (Fig. 8, C). While for the other sets of simulated profiles ($B_1(P), B_z(P), B(P)$ at $z_a=1$, and $B_z(P), B(P)$ at $z_a=4$) rise in pH led to increase in the extent of binding (notably, that without steepening of the curves), concentration of bound monomers exhibited pH-induced decrease in the presence of protein.

Similar effect was observed at varying ionic strength — only $B_1(L)$ and $B_1(P)$ dependencies undergo noteworthy modifications at $z_a=4$. While all other curves showed decreasing protein membrane affinity, as expected for electrostatically controlled adsorption (Table 1), $B_1(L)$ dependency was found to convert from sigmoidal to Langmuir-like, and $B_1(P)$ tended to increase with elevating the ionic strength (Fig. 9, A, B). The former phenomenon can be interpreted in terms of reduced sensitivity of monomer adsorption isotherms to the formation of protein aggregates, as was indicated while discussing Figs. 4, B and 5, B. In the meantime, B_1 increase with ionic strength (Fig. 9, B)

together with pH-induced B_1 decrease at $z_a=4$ (Fig. 8, C) may be treated as hallmarks of protein aggregation, i.e. such anomalous changes in $B_1(P)$ behavior may occur exclusively when bound protein is represented not only by monomeric but also oligomeric species.

3.4. Comparison with the experimental results

In the following it seems of importance to compare the results presented here with experimental data. The validity of the approach employed has been demonstrated in our recent study into adsorption of cationic protein lysozyme onto the negatively charged lipid bilayers [34]. To track the protein membrane binding lysozyme was covalently labeled with fluorescein (Fl), environmentally sensitive fluorophore responding to membrane association by a decrease in fluorescence. The monomer binding curves were obtained by monitoring the changes in Fl fluorescence as a function of lipid concentration and membrane content of anionic phospholipids. The recovered conversion of the adsorption isotherms from Langmuir-like to sigmoidal upon increasing membrane charge was rationalized in terms of enhanced aggregation propensity of the bound protein.

Sigmoidality of the adsorption isotherms as a signature of protein aggregation was also postulated in the recent work of Hinderliter and May [35]. While examining the adsorption of

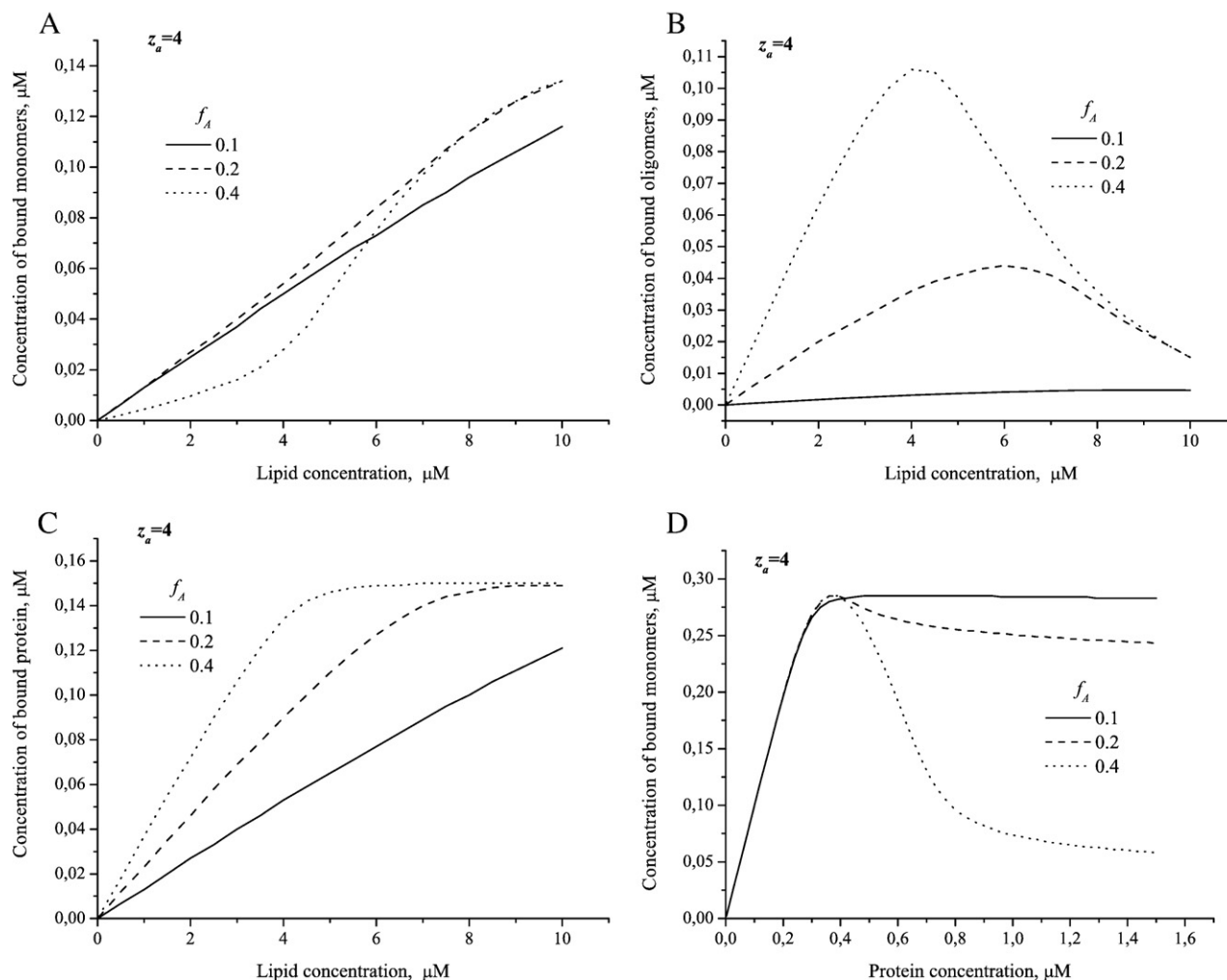


Fig. 6. Influence of bilayer surface charge density on monomer (A), (D) oligomer (B) and protein (C) binding curves for self-associating protein. Parameters used are: $n=10$, $K_0=10 \mu\text{M}$, $z=4$, $c=20 \text{ mM}$, $\text{pH}=7.4$, (A)–(C) $K_{12}=0.1$, $P=0.15 \mu\text{M}$, (D) — $K_{12}=10$, $L=20 \mu\text{M}$.

C2A domain of synaptotagmin onto the surface of anionic lipid vesicles the observed sigmoidal shape of $\Phi(F)$ binding curves was explained as arising from the formation of protein self-associates. The authors assert the aggregation to render the adsorption process cooperative, typical hallmark of which is the sigmoidal adsorption isotherms. Importantly, cooperativity of protein–lipid interactions may originate not only from protein–protein attraction but can also be mediated by structural reorganization of a lipid bilayer so that the shape of the binding isotherm may reflect the interplay between lateral membrane organization and surface coverage [36].

Cooperative bilayer interactions have been observed also for a number of peptides including antibiotic trichogin GA IV, antimicrobial peptide alamethicin, magainin [37–39]. The concentration of bound aggregates derived from oriented circular dichroism and time-resolved fluorescence data exhibited sigmoidal behavior being plotted as a function of total peptide concentration [37,38]. This finding is in harmony with our theoretical predictions (Fig. 2, B).

Analysis of the sets of binding curves obtained over a wide range of ionic strengths for the native and denatured

cytochrome *c* adsorbing onto the negatively charged lipid membranes led Heimburg and Marsh to conclusion about the enhanced tendency of the denatured protein to aggregate on the bilayer surface [13]. Although the derived $B(P)$ isotherms have typical Langmuir-like shape, it was shown that the binding curves for denatured protein can be fitted consistently to the Van der Waals gas adsorption model allowing for electrostatic effects only provided that the parameter describing protein–protein interactions takes nonzero positive value characteristic of the formation of protein aggregates.

Evidence for oligomerization of two specimens of cytochrome P450 protein superfamily at bilayer surface comes from the comprehensive study by Ramsden et al. [40]. More specifically, based on the results of integrated optics reflectance technique it was shown that RSA kinetics of protein adsorption is typical for the monomeric protein species while the Langmuir kinetics is indicative of protein clustering.

These examples illustrate that the different types of binding assays can provide arguments in favor of protein aggregation, especially if the shape of adsorption isotherms is analyzed over a range of experimental variables.

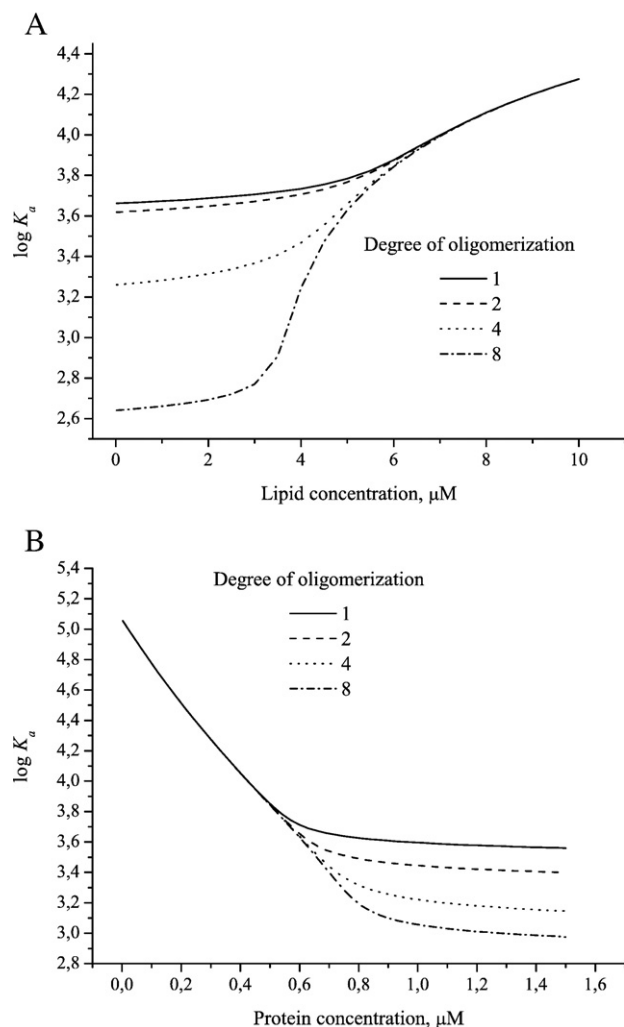


Fig. 7. Association constants as a function of lipid (A) or protein (B) concentration. Parameters used in simulation procedure are: $n=10$, $K_0=10 \mu\text{M}$, $z=4$, $f_A=0.4$, $c=20 \text{ mM}$, $\text{pH}=7.4$, (A) — $K_{1z}=0.1$, $P=0.15 \mu\text{M}$, (B) — $K_{1z}=10$, $L=20 \mu\text{M}$.

In the end, it seems of importance to emphasize that the adsorption model presented here was chosen as reasonable compromise between the complexity of the employed theoretical approaches and their ability to reflect the most general tendencies of the protein aggregation behavior at a surface. Clearly, any model may suffer from ignoring one or another factor. Specifically, in the present study electrostatic component of binding constant was derived assuming uniform charge distribution over the protein surface [19,41]. Although being oversimplified, this approach is currently widespread and in a number of cases seems to be reasonable [13,30,34], because alternative fixed charge model [42] requires knowing the exact location of charged groups at the protein surface. In this case, in terms of Tanford–Kirkwood formalism total electrostatic free energy of a protein is calculated as a sum of the free energies of interactions between each pair of point charges [42]. Evidently, in clarifying the common properties of self-associating surface-bound proteins the concepts of uniform charge distribution and effective protein charge seem to be more rational than protein-

specific approach based on fixed charge model. In this context it is noteworthy that available data are suggestive of insignificant differences between protein electrostatic free energies computed

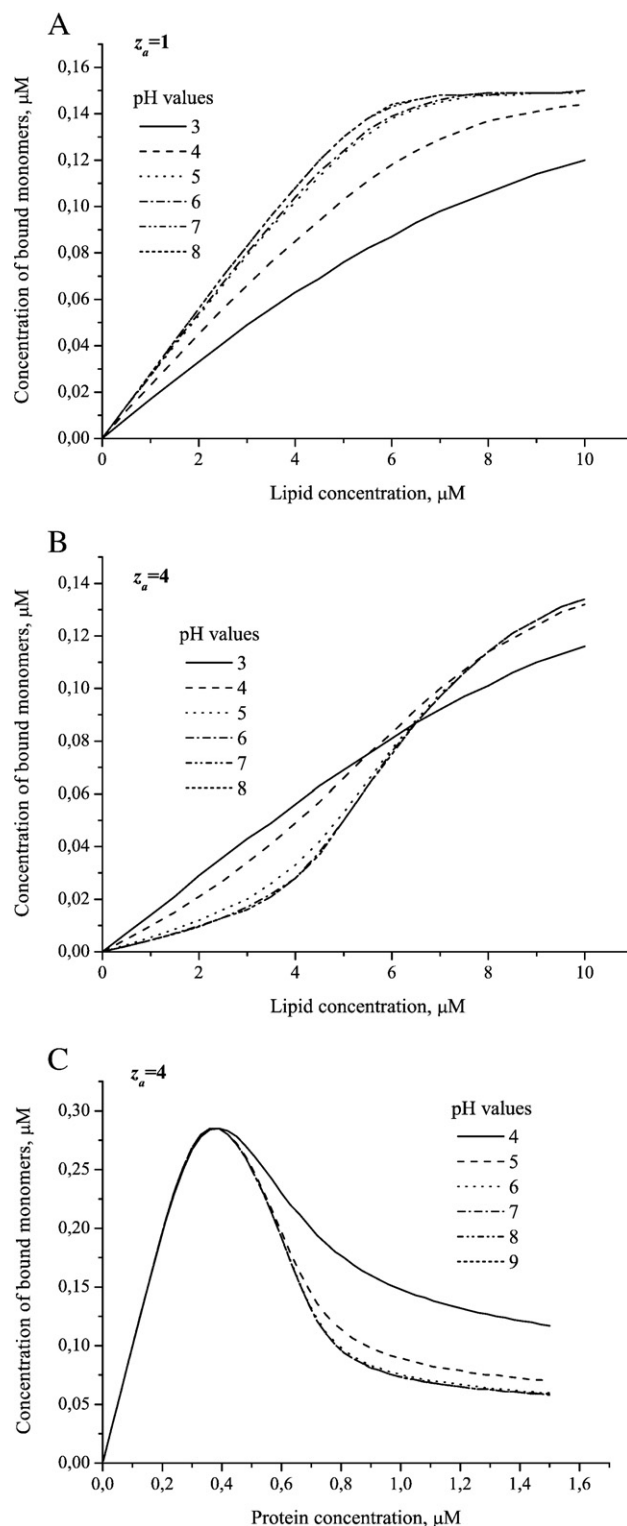


Fig. 8. pH effect on the behavior of adsorption isotherms: (A), (B) — constant protein concentration, $n=10$, $K_0=10 \mu\text{M}$, $K_{1z}=0.1$, $z=4 \text{ mM}$, $f_A=0.4$, $c=20 \text{ mM}$, $P=0.15 \mu\text{M}$, (C) — constant lipid concentration, $n=10$, $K_0=10 \mu\text{M}$, $K_{1z}=10$, $f_A=0.4$, $c=20 \text{ mM}$, $L=20 \mu\text{M}$.

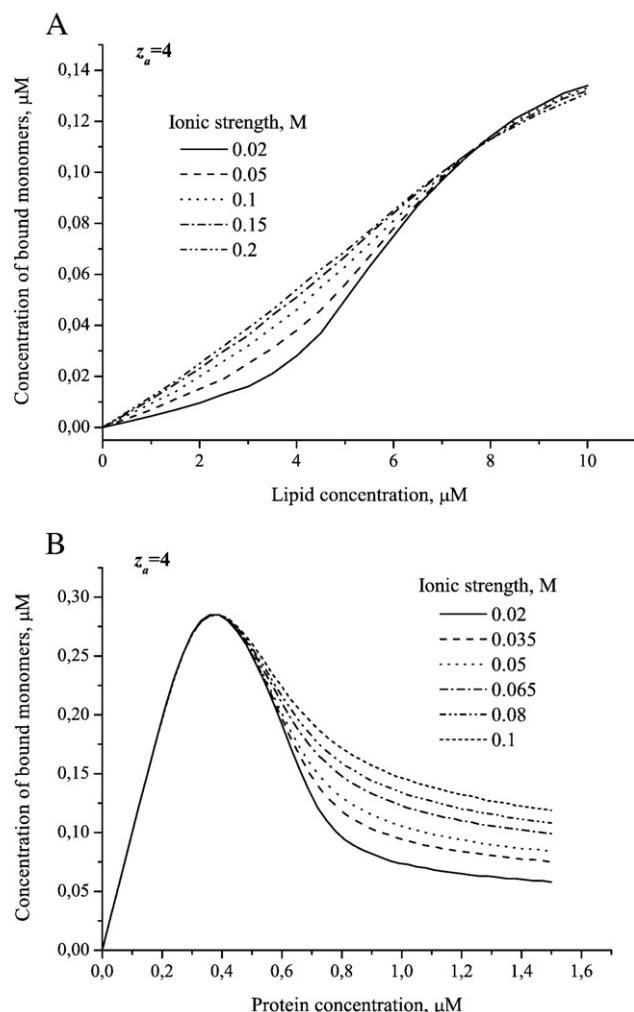


Fig. 9. Monomer binding curves at varying ionic strength for self-associating protein. Parameters used are: $n=10$, $K_0=10 \mu\text{M}$, $z=4$, $c=20 \text{ mM}$, $\text{pH}=7.4$, (A) — $K_{1z}=0.1$, $P=0.15 \mu\text{M}$, (B) — $K_{1z}=10$, $L=20 \mu\text{M}$.

by the smeared and fixed charge models. This was demonstrated, particularly, while calculating the titration curves of lysozyme where accurate consideration of charged group locations at the protein surface yields the free energy values close to those obtained assuming uniform charge distribution [43]. Based on the above rationales, in the present study the protein-unspecific smeared charge model was chosen as being the most appropriate to achieve the targeted goals.

Another point ignored in the adsorption model employed here concerns the possibility of multiple surface conformations of the adsorbed protein. Different types of surfaces have been reported to promote protein conformation changes leading to unfolding or denaturation of the protein molecule [44–48]. As follows from the semiempirical model proposed in fundamental work of Fernandez and Ramsden, surface-induced denaturation of folded proteins is driven by the lack of compensation between enthalpy loss associated with the formation of intramolecular and intermolecular protein–lipid contacts, and entropic penalty [49]. Accordingly, adsorbed protein may adopt more than a single conformation [50,51]. Such a possibility is allowed for in

SPT models by introducing distinct footprints for different adsorbate conformations [18,52]. In the simplest case two conformational states are considered — “end-on” with a square-of-circle-like projected contact area, and “side-on” with rectangular or elliptical projected contact area [18]. Random sequential adsorption (RSA) model treats conformational changes of adsorbing protein as spreading events [53,54] accompanied by the increase in protein size. As was demonstrated in our previous study the existence of multiple protein conformations *per se* cannot ensure the sigmoidal shape of adsorption isotherms [34]. In simulation studies the conversion of Langmuir-like binding curves to sigmoid-shaped was achieved only under assumption that at least one conformer undergoes self-association (data not shown) [14]. For these reasons, in identifying the typical signatures of protein aggregation at lipid–water interface we found it unreasonable to complicate the model by introducing the additional parameters characterizing multiple conformational states of a protein.

4. Conclusions

Cumulatively, comparison of different types of adsorption isotherms led us to the following ideas concerning the optimal design of binding experiments aimed at gaining insight into the aggregation behavior of cationic protein adsorbed onto negatively charged membrane surface. In this regard, the binding curves reflecting the changes of monomer concentration appear to be most informative. More specifically, while analyzing the set of monomer adsorption isotherms obtained over a range of experimental variables such as protein and lipid concentration, protein charge, proportion of anionic membrane constituent, pH or ionic strength, the following characteristic features, highlighted in grey in Table 1, can be treated as the signs of protein self-association:

- sigmoidal ($P=\text{const}$, $L=\text{var}$) or bell-shaped ($L=\text{const}$, $P=\text{var}$) form of adsorption isotherms,
- conversion of the curves from sigmoidal (P — fixed) or bell-shaped (L — fixed) to Langmuir-like upon increasing protein charge,
- inverse transformation of the curve shape — from Langmuir-like either to sigmoidal (P — fixed) or bell-shaped (L — fixed) with increasing membrane charge density,
- change of $B_1(L)$ isotherm from Langmuir-like to sigmoidal at increasing pH,
- sigmoidal-to-Langmuir-like transformation of $B_1(P)$ binding curve upon elevation of ionic strength.

It should also be emphasized that if one observes sigmoidal or bell-shaped $B_1(L)$ or $B_1(P)$ dependencies, the conclusion about formation of protein oligomers can be made with a relatively high level of confidence. However, if the derived $B_1(L)$ or $B_1(P)$ isotherms have Langmuir-like form, before jumping at hasty conclusion about the absence of protein aggregation, it is necessary to test whether these curves keep their shape at varying experimental parameters (z , f_A , pH , c). If this is the case, protein self-associates are unlikely to form, otherwise — oligomers evidently exist.

Appendix A. General statements of scaled particle theory

Scaled particle theory (SPT) provides theoretical background of statistical mechanical description of thermodynamic properties of hard sphere fluid containing one or more components. The original SPT proposed by Lebowitz and co-workers [55,56] yields the work for creation a spherical cavity or arbitrary size in the one-component hard sphere system. While treating the adsorption phenomena this theory permits calculating the chemical potential of adsorbed ligand. The main statements of SPT formalisms as applied to protein adsorption can be written as follows.

Let 1 represents protein species of radius R_1 already adsorbed onto membrane surface, and 2 — protein species of radius R_2 tending to adsorb and possessing chemical potential

$$\mu^{\text{sol}} = \mu^{\text{sol},o} + kT \ln F \quad (\text{A1})$$

where $\mu^{\text{sol},o}$ and F are standard state chemical potential and concentration of 2, respectively, in solution. Because adsorbate molecules are impenetrable, steric repulsions between them impose geometrical constraints on the placement of additional molecule. For example, for two spheres of radius R the minimal distance between their centers is $2R$ (Fig. A1), and the area around the first sphere excluded for the location of the center of the second sphere is $\pi(2R)^2 - \pi R^2 = 3\pi R^2$.

The thermodynamical equilibrium that controls the adsorption of 2 on a membrane surface is represented by:

$$\mu^{\text{sol}} = \mu^{\text{surf}} \quad (\text{A2})$$

where μ^{surf} is chemical potential of adsorbed species 2 which consist of standard state chemical potential $\mu^{\text{surf},o}$, mixing entropy $kT \ln \Phi$ and work $W(R_2)$ required to place 2 into the fluid of 1:

$$\mu^{\text{surf}} = \mu^{\text{surf},o} + kT \ln \Phi + W(R_2). \quad (\text{A3})$$

Applying Widom's insertion theorem it follows that:

$$W(R_2) = kT \ln \frac{S}{S_{\text{free}}} = kT \ln \frac{1}{\alpha} \quad (\text{A4})$$

here S — total area of membrane surface free of any adsorbed species, S_{free} — area of membrane surface available for

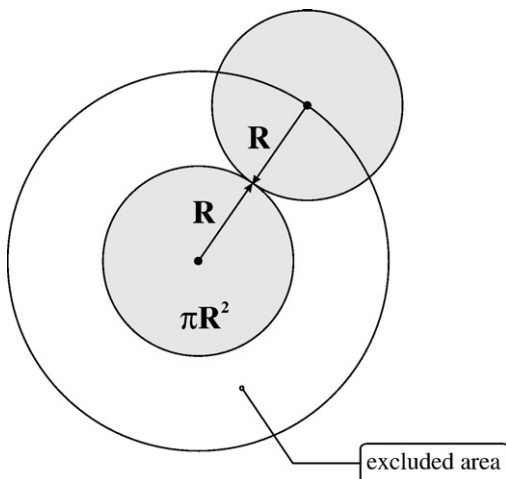


Fig. A1. Schematic representation of excluded area effect.

adsorption of species 2 when species 1 already adsorbed, α — free area (or volume) fraction which relates to activity coefficient of 2, γ , as:

$$\gamma = \alpha^{-1}. \quad (\text{A5})$$

Eq. (A3) thus can be rewritten as:

$$\mu^{\text{surf}} = \mu^{\text{surf},o} + kT \ln \Phi + kT \ln \gamma. \quad (\text{A6})$$

Denoting kT by β it is easy to show that:

$$-\ln \alpha = \ln \gamma = W(R_2)\beta. \quad (\text{A7})$$

On the hand, work W is defined as probability to find a cavity that is free of any part of 1 and into which 2 will be placed:

$$\beta W(R_2) = \ln P_o(R_2) \quad (\text{A8})$$

where

$$P_o(R_2) = 1 - P_1(R_2) \quad (\text{A9})$$

here $P_1(R_2)$ stands for the probability that 1 will be within the so-called co-area of species 1 and 2 (or the area excluded to the centers of 2 by centers of 1 averaged over all relative orientations of 1 and 2), A :

$$P_1(R_2) = \rho_1 A \quad (\text{A10})$$

ρ_1 — surface number density of 1, $A = \alpha_1 R_1^2 + c_1 c_2 R_1 R_2 / 2\pi$ [57], $c_{1,2} = C_{1,2} / R_{1,2}$, $\alpha_{1,2} = A_{1,2} / R_{1,2}^2$, $C_{1,2}$ and $A_{1,2}$ are circumference and area of 1 and 2, respectively.

Assuming that i) at $R_2=0$ $W(R_2)$ and $dW(R_2)/dR_2$ are continuous, ii) at $R_2 \rightarrow \infty$ $\lim W(R_2) = PA_2$, where P — is the pressure, the expression for $\beta W(R_2)$ takes the form:

$$\beta W(R_2) = \beta W(R_2 = 0) + \left(\frac{d\beta W(R_2 = 0)}{dR_2} \right) R_2 + \beta P a_2 R_2^2 \quad (\text{A11})$$

The pressure can be determined using the SPT equation of state for 2D convex particle of type 2 [57]:

$$\beta P = \rho_1 \left(\frac{1 + (\varepsilon - 1)\Phi}{(1 - \Phi)^2} \right) \quad (\text{A12})$$

where $\varepsilon = \frac{c_2^2}{4\pi a_1}$, $\Phi = \rho_1 A_1$.

Finally, one obtains:

$$\ln \gamma = -\ln(1 - \Phi) + 2\varepsilon f_c f_R \frac{\Phi}{1 - \Phi} + f_a f_R^2 \Phi \left(\frac{1 + (\varepsilon - 1)\Phi}{(1 - \Phi)^2} \right) \quad (\text{A13})$$

here $f_c = c_2/c_1$, $f_a = a_2/a_1$, $f_R = R_2/R_1$.

The expression for protein adsorption isotherm in the simplest case is:

$$K_a F = \Phi \gamma(\Phi). \quad (\text{A14})$$

In the case of self-associating protein, the chemical potential should be given both for adsorbed monomers (μ_1^{surf}) and z_a -mers (μ_z^{surf}). Analogously to Eq. (A6) one can write [14]:

$$\mu_1^{\text{surf}} = \mu_1^{\text{surf},o} + kT \ln \Phi_1 + kT \ln \gamma_1(\Phi_1, \Phi_z) \quad (\text{A15a})$$

$$\mu_z^{\text{surf}} = \mu_z^{\text{surf},o} + kT \ln \Phi_z + kT \ln \gamma_z(\Phi_1, \Phi_z) \quad (\text{A15b})$$

Equilibrium conditions $\mu_1^{\text{sol}} = \mu_1^{\text{surf}}$, $z\mu_1^{\text{sol}} = \mu_z^{\text{surf}}$ result to the Eqs. (1)–(4) describing the adsorption isotherms for self-associating ligand [14,57].

References

- [1] H. Zhao, E.K.J. Tuominen, P.K.J. Kinnunen, Formation of amyloid fibers triggered by phosphatidylserine-containing membranes, *Biochemistry* 43 (2004) 10302–10307.
- [2] G.P. Gorbenko, P.K.J. Kinnunen, The role of lipid–protein interactions in amyloid-type protein fibril formation, *Chem. Phys. Lipids* 141 (2006) 72–82.
- [3] C.M. Dobson, The structural basis of protein folding and its links with human disease, *Philos. Trans. R. Soc. Lond. Ser. B* 356 (2001) 133–145.
- [4] J.D. Knight, A.D. Miranker, Phospholipid catalysis of diabetic amyloid assembly, *J. Mol. Biol.* 341 (2004) 1175–1187.
- [5] P. Devaux, M. Seigneuret, Specificity of lipid–protein interactions as determined by spectroscopic techniques, *Biochim. Biophys. Acta* 822 (1985) 63–125.
- [6] K. Peng, A.J.W.G. Visser, A. van Hoek, C.J.A.M. Wolfs, M.A. Hemminga, Analysis of time-resolved fluorescence anisotropy in lipid–protein systems, *Eur. Biophys. J.* 18 (1990) 285–293.
- [7] M. Lindgren, K. Sorgjerd, P. Hammarstrom, Detection and characterization of aggregates, prefibrillar amyloidogenic oligomers, and protofibrils using fluorescence spectroscopy, *Biophys. J.* 88 (2005) 4200–4212.
- [8] M. Calamai, C. Canale, A. Relini, M. Stefani, F. Chiti, C.M. Dobson, Reversal of protein aggregation provides evidence for multiple aggregated states, *J. Mol. Biol.* 346 (2005) 603–616.
- [9] C.A. Hasselbacher, T.L. Street, T.G. Dewey, Resonance energy transfer as a monitor of membrane protein domain segregation: application to the aggregation of bacteriorhodopsin reconstituted into phospholipid vesicles, *Biochemistry* 23 (1984) 6445–6452.
- [10] S. Stankowski, Large ligand adsorption to membranes. I. Linear ligands as a limiting case, *Biochim. Biophys. Acta* 735 (1983) 341–351.
- [11] S. Stankowski, Large ligand adsorption to membranes. II. Disc-like ligands and shape dependence at low saturation, *Biochim. Biophys. Acta* 735 (1983) 352–360.
- [12] S. Stankowski, Large ligand adsorption to membranes. III. Cooperativity and general ligand shapes, *Biochim. Biophys. Acta* 777 (1984) 167–182.
- [13] T. Heimburg, D. Marsh, Protein surface-distribution and protein–protein interactions in the binding of peripheral proteins to charged lipid membranes, *Biophys. J.* 68 (1995) 536–546.
- [14] R. Chatelier, A.P. Minton, Adsorption of globular proteins on locally planar surfaces: models for the effect of excluded surface area and aggregation of adsorbed protein on adsorption equilibria, *Biophys. J.* 71 (1996) 2367–2374.
- [15] J. Talbot, Molecular thermodynamics of binary mixture adsorption: a scaled particle theory approach, *J. Chem. Phys.* 106 (1997) 4696–4706.
- [16] K. Al-Malah, J. McGuire, R. Sproull, A macroscopic model for the single-component protein adsorption isotherm, *J. Colloid Interface Sci.* 170 (1995) 261–268.
- [17] M. Wahlgren, U. Elofsson, Simple models for adsorption kinetics and their correlation to the adsorption of β -lactoglobulin A and B, *J. Colloid Interface Sci.* 188 (1997) 121–129.
- [18] A. Minton, Adsorption of globular proteins on locally planar surfaces. II. Models for the effect of multiple adsorbate conformations on adsorption equilibria and kinetics, *Biophys. J.* 76 (1999) 176–187.
- [19] C. Tanford, The electrostatic free energy of globular protein ions in aqueous solution, *J. Phys. Chem.* 59 (1955) 788–793.
- [20] F. Jahng, Electrostatic free energy and shift of the phase transition for charged lipid membranes, *Biophys. Chem.* 4 (1976) 309–318.
- [21] O.G. Mouritsen, Theoretical models of phospholipid phase transitions, *Chem. Phys. Lipids* 57 (1991) 179–194.
- [22] J.Y.A. Lehtonen, J.M. Holopainen, P.K.J. Kinnunen, Evidence for the formation of microdomains in liquid crystalline large unilamellar vesicles caused by hydrophobic mismatch of the constituent phospholipids, *Biophys. J.* 70 (1996) 1753–1760.
- [23] O.G. Mouritsen, M. Bloom, Mattress model of lipid–protein interactions in membranes, *Biophys. J.* 46 (1994) 141–153.
- [24] J.M. Holopainen, M. Subramanian, P.K.J. Kinnunen, Sphingomyelinase induces lipid microdomain formation in a fluid phosphatidylcholine/sphingomyelin membrane, *Biochemistry* 37 (1998) 17562–17570.
- [25] M. Rytomaa, P.K.J. Kinnunen, Dissociation of cytochrome c from liposomes by histone H1. Comparison with basic peptides, *Biochemistry* 35 (1996) 4529–4539.
- [26] T. Soderlund, A. Jutila, P.K.J. Kinnunen, Binding of adriamycin to liposomes as a probe for membrane lateral organization, *Biophys. J.* 76 (1999) 896–907.
- [27] M. Mosior, S. McLaughlin, Electrostatics and reduction of dimensionality produce apparent cooperativity when basic peptides bind to acidic lipids in membranes, *Biochim. Biophys. Acta* 1105 (1992) 185–187.
- [28] G. Denisov, S. Wanaski, P. Luan, M. Glaser, S. McLaughlin, Binding of basic peptides to membranes produces lateral domains enriched in the acidic lipids phosphatidylserine and phosphatidylinositol-4,5-bisphosphate: an electrostatic model and experimental results, *Biophys. J.* 74 (1998) 731–744.
- [29] T. Heimburg, B. Angerstein, D. Marsh, Binding of peripheral proteins to mixed lipid membranes: effect of lipid demixing upon binding, *Biophys. J.* 76 (1999) 2575–2586.
- [30] S. May, D. Harries, A. Ben-Shaul, Lipid demixing and protein–protein interactions in the adsorption of charged proteins on mixed membranes, *Biophys. J.* 79 (2000) 1747–1760.
- [31] E.C. Mbamala, A. Ben-Shaul, S. May, Domain formation induced by the adsorption of charged proteins on mixed lipid membranes, *Biophys. J.* 88 (2005) 1702–1714.
- [32] J. Tocanne, J. Teissie, Ionization of phospholipids and phospholipid-supported interfacial lateral diffusion of protons in membrane model systems, *Biochim. Biophys. Acta* 1031 (1990) 111–142.
- [33] M. Kates, J. Syz, D. Gosser, T.H. Haines, pH-dissociation characteristics of cardiolipin and its 29-deoxy analogue, *Lipids* 28 (1993) 877–882.
- [34] G.P. Gorbenko, V.M. Ioffe, P.K.J. Kinnunen, Binding of lysozyme to phospholipid bilayers: evidence for protein aggregation upon membrane association, *Biophys. J.* 93 (2007) 140–153.
- [35] A. Hinderliter, S. May, Cooperative adsorption of proteins onto lipid membranes, *J. Phys., Condens. Matter* 18 (2006) S1257–S1270.
- [36] M.S. Wooster, J.M. Wigglesworth, Adsorption of glyceraldehyde 3-phosphate dehydrogenase on condensed monolayers of phospholipid, *Biochem. J.* 153 (1976) 93–100.
- [37] L. Stella, C. Mazzuca, M. Venanzi, A. Palleschi, M. Didone, F. Formaggio, C. Toniolo, B. Pispisa, Aggregation and water-membrane partition as major determinants of the activity of the antibiotic peptide trichogin GA IV, *Biophys. J.* 86 (2004) 936–945.
- [38] F.Y. Chen, M.T. Lee, H.W. Huang, Sigmoidal concentration dependence of antimicrobial peptide activities: a case study of alamethicin, *Biophys. J.* 82 (2002) 908–914.
- [39] S.J. Ludtke, K. He, Y. Wu, H.W. Huang, Cooperative membrane insertion of magainin correlated with its cytolytic activity, *Biochim. Biophys. Acta* 1190 (1994) 181–184.
- [40] J.J. Ramsden, G.I. Bachmanova, A.I. Archakov, Kinetic evidence for protein clustering at a surface, *Phys. Rev., E* 50 (1994) 5072–5076.
- [41] K. Linderström-Lang, The ionization of proteins, *C.R. Trav. Lab. Carlsberg* 15 (1924) 1–29.
- [42] C. Tanford, J.G. Kirkwood, Theory of protein titration curves. I. General equations for impenetrable sphere, *J. Am. Chem. Soc.* 79 (1957) 5333–5339.
- [43] T. Imoto, Electrostatic free energy of lysozyme, *Biophys. J.* 44 (1983) 293–298.

- [44] D.M. Hylton, S.W. Shalaby, R.A. Latour, Direct correlation between adsorption-induced changes in protein structure and platelet adhesion, *J. Biomed. Mater. Res.*, A 73 (2005) 349–358.
- [45] K.L. Marchin, C.L. Berrie, Conformational changes in the plasma protein fibrinogen upon adsorption to graphite and mica investigated by atomic force microscopy, *Langmuir* 19 (2003) 9883–9888.
- [46] A. Kondo, F. Murakami, K. Higashitani, Circular dichroism studies on conformational changes in protein molecules upon adsorption on ultrafine polystyrene particles, *Biotechnol. Bioeng.* 40 (2004) 889–894.
- [47] M.F.M. Engel, C.P.M. van Mierlo, A.J.W.G. Visser, Kinetic and structural characterisation of adsorption induced unfolding of bovine α -lactalbumin, *J. Biol. Chem.* 277 (2002) 10922–10930.
- [48] N. Sanghera, T.J.T. Pinheiro, Unfolding and refolding of cytochrome *c* driven by the interaction with lipid micelles, *Prot. Sci.* 9 (2000) 1194–1202.
- [49] A. Fernandez, J. Ramsden, On adsorption-induced denaturation of folded proteins, *J. Biol. Phys. Chem.* 1 (2001) 81–84.
- [50] E. Brynda, M. Houska, F. Lednický, Adsorption of human fibrinogen onto hydrophobic surfaces: the effect of concentration in solution, *J. Colloid Interface Sci.* 113 (1986) 164–171.
- [51] M. Wahlgren, T. Arnebrant, I. Lundström, Adsorption of lysozyme to hydrophilic silicon oxide surfaces: comparison between experimental data and models for adsorption kinetics, *J. Colloid Interface Sci.* 175 (1995) 506–514.
- [52] X. Jin, Z. Ma, J. Talbot, N.H.L. Wang, A model for the adsorption equilibria of solutes with multiple adsorption orientations, *Langmuir* 15 (1999) 3321–3333.
- [53] P.R. Van Tassel, P. Viot, G. Tarjus, J.J. Ramsden, J. Talbot, Enhanced saturation coverages in adsorption–desorption processes, *J. Chem. Phys.* 112 (2000) 1483–1488.
- [54] P.R. Van Tassel, P. Viot, G. Tarjus, J. Talbot, Irreversible adsorption of macromolecules at a liquid–solid interface: theoretical studies of the effects of conformational change, *J. Chem. Phys.* 101 (1994) 7064–7073.
- [55] H. Reiss, H.L. Frisch, J.L. Lebowitz, Statistical mechanics of rigid spheres, *J. Chem. Phys.* 31 (1959) 369–380.
- [56] J.L. Lebowitz, E. Helfand, E. Praestgaard, Scaled particle theory of fluid mixtures, *J. Chem. Phys.* 43 (1965) 774–779.
- [57] T. Boublik, Two-dimensional convex particle liquid, *Mol. Phys.* 29 (1975) 421–428.